Acknowledgements

We thank B. H. Mauk, S. Krimigis, W. S. Kurth and M. Kaiser for helpful discussions. The support of the Chandra Project and the Smithsonian Astrophysical Observatory is gratefully acknowledged. A portion of this work is based on observations made with the NASA/ESA Hubble Space Telescope, obtained at the Space Telescope Science Institute, which is operated by the Association of Universities for Research in Astronomy, Inc.

Correspondence and requests for materials should be addressed to G.R.G. (e-mail: randy@whistler.space.swri.edu).

Transient aurora on Jupiter from injections of magnetospheric electrons

B. H. Mauk*, J. T. Clarke†, D. Grodent‡, J. H. Waite Jr‡, C. P. Paranicas* & D. J. Williams*

* *The Johns Hopkins University Applied Physics Laboratory, 11100 Johns Hopkins Road, Laurel, Maryland 20723, USA*
† *Department of Astronomy and Center for Space Physics, Boston University, 725 Commonwealth Avenue, Boston, Massachusetts 02215, USA*
‡ *Department of Atmospheric, Oceanic, and Space Sciences, University of Michigan, Ann Arbor, Michigan 48109, USA*

Energetic electrons and ions that are trapped in Earth's magnetosphere can suddenly be accelerated towards the planet[1–5]. Some dynamic features of Earth's aurora (the northern and southern lights) are created by the fraction of these injected particles that travels along magnetic field lines and hits the upper atmosphere[4]. Jupiter's aurora appears similar to Earth's in some respects; both appear as large ovals circling the poles and both show transient events[6–11]. But the magnetospheres of Jupiter and Earth are so different—particularly in the way they are powered—that it is not known whether the magnetospheric drivers[12] of Earth's aurora also cause them on Jupiter. Here we show a direct relationship between Earth-like injections of electrons in Jupiter's magnetosphere and a transient auroral feature in Jupiter's polar region. This relationship is remarkably similar to what happens at Earth, and therefore suggests that despite the large differences between planetary magnetospheres, some processes that generate aurorae are the same throughout the Solar System.

The injections within Earth's magnetosphere (Fig. 1) involve particles with kilo-electron volt (keV) to mega-electron volt (MeV) energies[4]. Often occurring at radial distances of 6 to 10 Earth radii, injections are one component of global dynamic events called 'magnetospheric substorms'. Substorms represent, in part, the transient release of energy stored in the magnetosphere with stressed magnetic fields[13]. The energy source for Earth's substorms is the solar wind of charged gases, or plasmas, emanating from the Sun. Substorms create dramatic brightening of the aurora at high geographic latitudes and a substantial expansion of the regions where auroral emissions occur.

The recent discovery of Earth-like charged particle injections within Jupiter's magnetosphere[14,15] is surprising because Jupiter's magnetosphere is powered mostly from the inside by the rapid but steady planetary rotation rather than from the outside by the variable solar wind. The role of injections in generating auroral emissions at Jupiter has been heretofore unknown, to our knowledge.

A unique opportunity to address dynamics in Jupiter's space environment was made available by a Jupiter joint observation campaign in late 2000 and early 2001. It involved the fly-by of the Cassini spacecraft, headed toward Saturn, the Galileo spacecraft orbiting Jupiter, and remote imaging by the Hubble Space Telescope (HST). During the campaign, Galileo recorded energetic electron injection signatures at radial distances of ~10 to ~13 Jupiter radii (Fig. 2). A simple model (Fig. 3) explains the energy-dispersed character of these signatures (different particle energies arrived at Galileo at different times). The model is closely analogous to models derived from injections at Earth[16–18]. Quantitative analysis (Fig. 4) reveals the temporal relationship between the injections and the signatures. At the times of the injections, around 15 h before the dispersed signatures were observed, Galileo was at a radial distance of about 20 Jupiter radii and recorded no obvious signature of the injections occurring closer to Jupiter.

Ultraviolet HST auroral images, similar to those in previous reports[7], were taken during the Galileo operations and remapped to polar coordinates (Fig. 5). The images reveal a distinct auroral emission patch in eight consecutive images (100-s exposures)

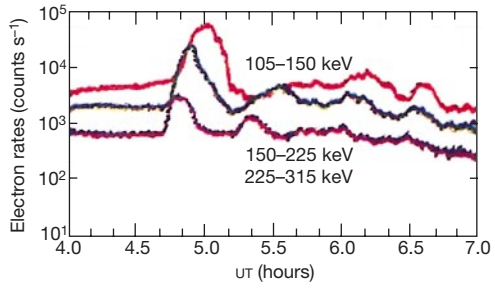

Figure 1 Energetic electron injection measurements within Earth's space environment. The response of three different electron energy channels is shown as measured from the Earth's geosynchronous orbit (~6.7 Earth radii circular, near-equatorial). We note the energy-dispersed nature of the channels, with different energies arriving at the spacecraft at different times. Plotted after ref. 5.

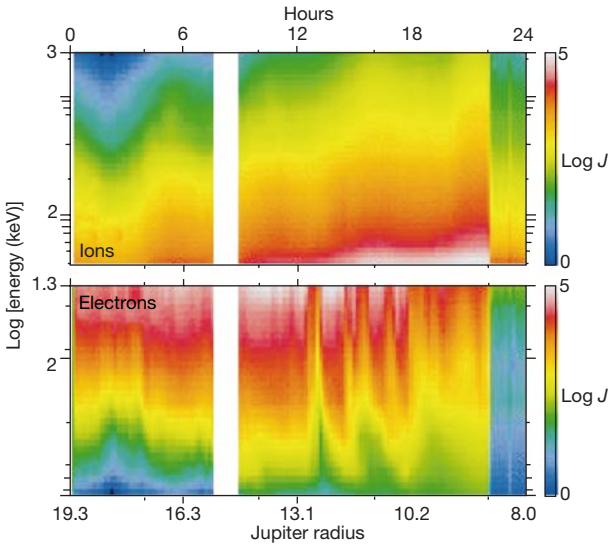

Figure 2 Energetic electron injection measurements within Jupiter's magnetosphere. Log [energy (keV)] versus time (hours of day 363, 2000; top scale) versus particle log [intensity (cm^{-1} s^{-1} sr^{-1} keV^{-1}], shown as a colour scale, display of ion (top) and electron (bottom) measurements from the energetic particle detector on the Galileo spacecraft for the radial range of 19 to 8 Jupiter radii (bottom scale). The energy-dispersed injections are visible in the right-hand portion of the electron display beginning at about hour 13. The electron sensor is nearly saturated at the lower energies (top of the electron display) and so the relative variations at low energies is underrepresented here.

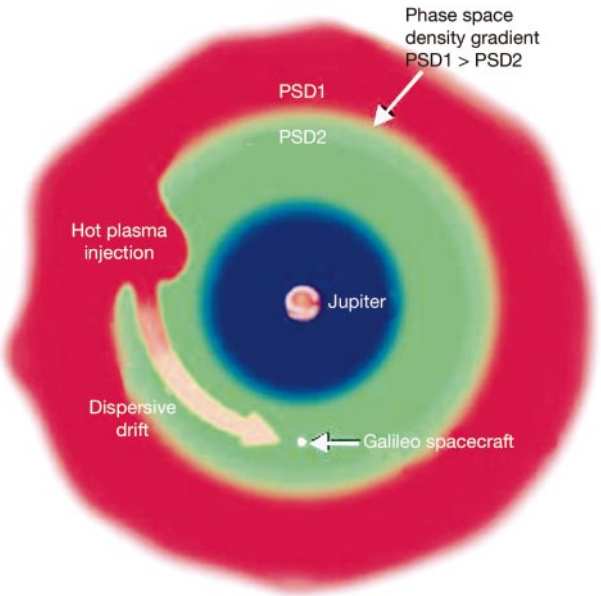

Figure 3 Schematic for the generation of injections within Jupiter's magnetosphere. The hot plasma injection (left side) occurs quickly, and then the dispersive drift, driven by Jupiter's rotation and magnetic field inhomogeneities, occurs slowly and generates energy-dispersed particle signatures at Galileo. The phase space density (PSD) is a transformation of the particle intensities into a form that is invariant for the kind of transport thought to occur here. Plotted after refs 14 and 15.

obtained over a 36-min HST operation period (Fig. 5, extreme right and close to the yellow square labelled '15 h'). The auroral patch moved with Jupiter as Jupiter rotated, and thus maintained its latitude–longitude position. The last image of the set was taken at about 1230 UT, about 30 min before the beginning of the first injection signature in Fig. 2.

We believe the patch was generated by the first of the injections

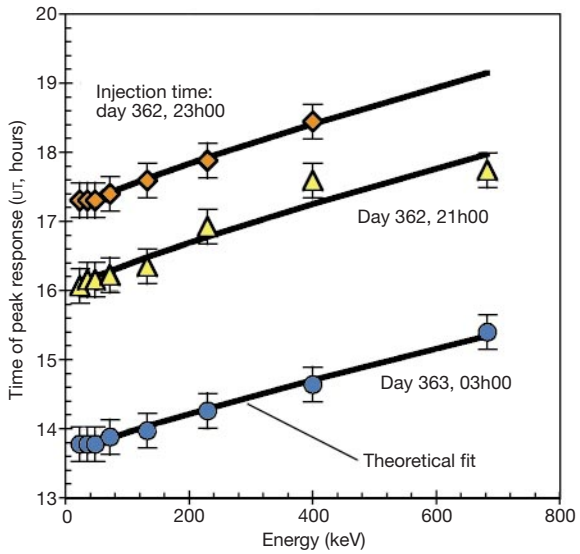

Figure 4 Quantitative analysis of Jupiter's energy-dispersed electron injection signatures. Plotted points are the times (hours in day 363 of 2000) versus energy of the peaks in the electron channel responses for the three main electron injection signatures shown in Fig. 2. The theoretical fits use the best estimates of the energy-dependent drifts within Jupiter's magnetosphere[15] to reconstruct the times (shown in the figure) when the fast injections (Fig. 3) occurred. These estimates make use of a magnetic field model that incorporates electric currents internal to Jupiter and the latest estimates of typical currents external to Jupiter within the magnetosphere[19].

observed by Galileo (Fig. 4). In Fig. 5, the yellow squares and the yellow dashed line show two different calculations of the motion of the Galileo spacecraft trajectory when mapped along magnetic field lines from the spacecraft to Jupiter's upper atmosphere. The yellow dashed line is the better estimate because the magnetic field model used to map Galileo's position includes contributions both from currents internal to Jupiter and from up-to-date estimates of average currents flowing external to Jupiter within its magnetosphere[19]. Adequate approximation to the magnetic field requires that external currents be included because the actual magnetic field configuration beyond about 9 Jupiter radii is distorted away from the nearly dipolar configuration expected from internal currents alone[19,20]. Projections derived using a field model with only internal currents (yellow squares in Fig. 5; VIP4[21]) are shown to provide a sense of the uncertainties involved with mapping. With the better estimate, the Galileo trajectory appears to have crossed into the isolated patch between ~14.7 and ~15.3 h, centred on the maximum of the higher-energy portion of the injection feature (Fig. 4). This result does not depend on detailed timing because, as mentioned, the auroral patch maintained its latitude–

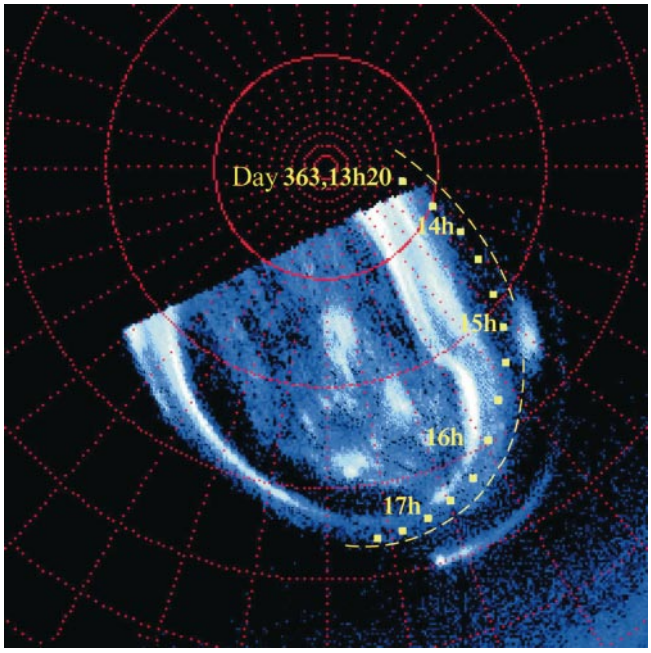

Figure 5 Hubble Space Telescope (HST) ultraviolet image of Jupiter's northern hemisphere aurora transformed to a Jupiter system-III polar coordinate system. Zero and 90 degree longitudes are straight up and horizontal to the right, respectively. The auroral emission patch of interest is to the extreme right, adjacent to the yellow square labelled '15 h'. The yellow squares and yellow dashed line show magnetic projections of the Galileo spacecraft onto Jupiter's upper atmosphere using two models of Jupiter's magnetic field (see text for details). The model of Khurana[19], that includes currents external to Jupiter, was updated by replacing the internal field model, O6, with the latest internal field model, VIP4[21]. We note that as Galileo moved closer to Jupiter, the trajectory appears to move closer and closer to the strong emissions of the bright, poleward ring of the auroral oval. Although this is not the subject of this Letter, this characteristic is contrary to what one might expect if this ring of emission has a source that predominates steadily at some radial distance. However, as verified with previous work (see Fig. 1 of ref. 9), present field models do not predict the poleward kink in the global auroral distribution of the brightest aurora, revealed here aligned along the 140–150° longitude meridian and in previous work[7]. The structure of the bright auroral oval is clearly different in the kink region from its structure elsewhere, and so more than just a refinement in magnetic mapping at high latitudes will be needed to understand it. Local time effects[6,9] and perhaps even the effects of dynamics may be involved here. The brightest aurora is thought to map to distances as large as ~20–30 Jupiter radii, and given the mapping sensitivities[9], our results are consistent with that hypothesis.

longitude position as Jupiter rotated.

The auroral patch characteristic of rotating with Jupiter is expected because the injected electrons also rotate with Jupiter (within several per cent at ~12 Jupiter radii[15]). Although the auroral patch of interest here was the brightest observed during the joint observation campaign, such patches are common within HST images. Likewise, the occurrence of jovian electron injections is also common[15]. The other energetic electron injections revealed in the Galileo data (Figs 2 and 4) map to regions (Fig. 5) that also show measurable auroral emissions. However, those emissions do not appear patch-like and may have been active even in the absence of injections.

Studies of Earth's magnetosphere[13] suggest two different ways that injected energetic particles can generate auroral emissions. (1) The particle energy distributions are modified during injection and become unstable to exchanges of energy with magnetospheric wave modes. The waves scatter particles so that some travel narrowly along the magnetic field lines until they encounter the atmosphere. (2) The injected particle cloud is a high-pressure region and so electric current flows along its boundary. This pressure-driven (diamagnetic) current diverges along the leading and trailing edges of the rotating cloud because the magnetic field strength changes with radial distance. Currents are driven along the magnetic field lines towards and away from the planet and can interact strongly with plasmas close to the planet. At Jupiter, that interaction would yield downward accelerated electrons, and atmospheric auroral emissions, at the trailing edge of the rotating plasma cloud. Although there is substantial uncertainty in the magnetic mapping, the position of the auroral patch does match best with either the trailing edge of the electron cloud (the second mechanism) or the centre of that portion of the cloud that contained the higher-energy electrons measured (the first mechanism).

For an aurora resulting from the scattering process, the maximum power density that the measured (>20 keV) electron cloud can provide to the aurora is $60 \pm 30\,\mathrm{erg\,cm^{-2}\,s^{-1}}$. Higher power densities are possible with the electric current generation mechanism. Models of interaction between electrons and Jupiter's atmosphere[22], recalculated with the energy distribution shapes measured in Fig. 2, yield about $3\,\mathrm{erg\,cm^{-2}\,s^{-1}}$ for the electron input needed to explain the auroral emissions. Thus, measured electrons can supply the requisite energy with scattering efficiencies of only 3% to 10% of the maximum. Auroral optical emission spectra were not available for this event to estimate independently the electron energies involved. However, recent Galileo auroral observations measured the tangent altitude (above the 1-bar atmospheric pressure level) of peak auroral emissions at 245 ± 30 km, with some emissions extending to an altitude of 120 ± 40 km (ref. 23). Atmospheric penetration of electrons modelled for diffuse aurorae require the involvement of over 48 keV electrons to explain even the peak auroral emissions[24,22]. □

Received 8 November 2001; accepted 1 February 2002.

1. Konradi, A. Proton events in the magnetosphere associated with magnetic bays. *J. Geophys. Res.* **72,** 3829–3841 (1967).
2. Arnoldy, R. L. & Chan, K. W. Particle substorms observed at the geostationary orbit. *J. Geophys. Res.* **74,** 5019–5028 (1969).
3. DeForest, S. E. & McIlwain, C. E. Plasma clouds in the magnetosphere. *J. Geophys. Res.* **76,** 3587–3611 (1971).
4. Mauk, B. H. & Meng, C.-I. in *Auroral Physics* (eds Meng, C.-I., Rycroft, M. J. & Frank, L. A.) 223–240 (Cambridge Univ. Press, Cambridge, 1991).
5. Li, X. *et al.* Simulation of dispersionless injections and drift echos of energetic electrons associated with substorms. *Geophys. Res. Lett.* **25,** 3763–3766 (1998).
6. Satoh, T., Connerney, J. E. P. & Baron, R. L. Emission source model of Jupiter's H_3^+ aurorae: A generalized inverse analysis of images. *Icarus* **122,** 1–23 (1996).
7. Clarke, J. T. *et al.* Far-ultraviolet imaging of Jupiter's aurora and the Io "footprint". *Science* **274,** 404–409 (1996).
8. Ballester, G. E. *et al.* Time-resolved observations of Jupiter's far-ultraviolet aurora. *Science* **274,** 409–413 (1996).
9. Satoh, T. & Connerney, J. E. P. Jupiter's H_3^+ emissions viewed in corrected jovimagnetic coordinates. *Icarus* **141,** 236–252 (1999).
10. Waite, J. H. *et al.* Multispectral observations of Jupiter's aurora. *Adv. Space Res.* **26,** 1453–1475 (2000).
11. Waite, J. H. *et al.* An auroral flare at Jupiter. *Nature* **410,** 787–789 (2001).
12. Meng, C.-I., Rycroft, M. J. & Frank, L. A. *Auroral Physics* (Cambridge Univ. Press, Cambridge, 1991).
13. Kivelson, M. G. & Russell, C. T. (eds) *Introduction to Space Physics* (Cambridge Univ. Press, Cambridge, 1995).
14. Mauk, B. H., Williams, D. J. & McEntire, R. W. Energy-time dispersed signatures of dynamic injections in Jupiter's inner magnetosphere. *Geophys. Res. Lett.* **24,** 2949–2953 (1997).
15. Mauk, B. H. *et al.* Storm-like dynamics of Jupiter's inner magnetosphere. *J. Geophys. Res.* **104,** 22759–22778 (1999).
16. McIlwain, C. E. in *Earth's Magnetospheric Processes* (ed. McCormac, B. M.) 268–279 (Reidel, Hingham, 1972).
17. Konradi, A., Semar, C. L. & Fritz, T. A. Substorm-injected protons and electrons and the injection boundary model. *J. Geophys. Res.* **80,** 543–552 (1975).
18. Mauk, B. H. & Meng, C.-I. Characterization of geostationary particle signatures based on the 'injection boundary model'. *J. Geophys. Res.* **88,** 3055–3071 (1983).
19. Khurana, K. K. Euler potential models of Jupiter's magnetospheric field. *J. Geophys. Res.* **102,** 11295–11306 (1997).
20. Connerney, J. E. P., Acuña, M. H. & Ness, N. F. Modeling the jovian current sheet and inner magnetosphere. *J. Geophys. Res.* **86,** 8370–8384 (1981).
21. Connerney, J. E. P. *et al.* New models of Jupiter's magnetic field constrained by the Io flux tube footprint. *J. Geophys. Res.* **103,** 11929–11939 (1998).
22. Grodent, D., Waite, J. H. Jr & Gérard, J.-C. A self-consistent model of the jovian auroral thermal structure. *J. Geophys. Res.* **106,** 12933–12952 (2001).
23. Vasavada, A. R. *et al.* Jupiter's visible aurora and Io footprint. *J. Geophys. Res.* **104,** 27133–27142 (1999).
24. Ajello, J. *et al.* Galileo orbiter ultraviolet observations of Jupiter aurora. *J. Geophys. Res.* **103,** 20125–20148 (1998).

Acknowledgements

We gratefully acknowledge help from and discussions with R. W. McEntire and T. Choo, and the support of the Space Telescope Institute.

Competing interests statement

The authors declare that they have no competing financial interests.

Correspondence and requests for materials should be addressed to B.H.M. (e-mail: Barry.Mauk@jhuapl.edu).

Bandgap modulation of carbon nanotubes by encapsulated metallofullerenes

Jhinhwan Lee*†, H. Kim*†, S.-J. Kahng‡, G. Kim*, Y.-W. Son*, J. Ihm*, H. Kato§, Z. W. Wang§, T. Okazaki§, H. Shinohara§ & Young Kuk*†

** School of Physics and † Center for Science in Nanometer Scale, Seoul National University, Seoul 151-747, Korea*
‡ Department of Physics, Soongsil University, Seoul 156-743, Korea
§ Department of Chemistry, Nagoya University, Nagoya 464-8602, Japan

Motivated by the technical and economic difficulties in further miniaturizing silicon-based transistors with the present fabrication technologies, there is a strong effort to develop alternative electronic devices, based, for example, on single molecules[1,2]. Recently, carbon nanotubes have been successfully used for nanometre-sized devices such as diodes[3,4], transistors[5,6], and random access memory cells[7]. Such nanotube devices are usually very long compared to silicon-based transistors. Here we report a method for dividing a semiconductor nanotube into multiple quantum dots with lengths of about 10 nm by inserting $Gd@C_{82}$ endohedral fullerenes. The spatial modulation of the nanotube electronic bandgap is observed with a low-temperature scanning tunnelling microscope. We find that a bandgap of ~0.5 eV is narrowed down to ~0.1 eV at sites where endohedral metallofullerenes are inserted. This change in bandgap can be explained by local elastic strain and charge transfer at metallofullerene sites. This technique for fabricating an array of quantum dots could be used for nano-electronics[8] and nano-optoelectronics[9].